35th Annual International Conference of the IEEE EMBS
Osaka, Japan, 3 - 7 July, 2013

A Model of Evoked Potentials in Spinal Cord Stimulation

James H. Laird[1,2] and John L. Parker[1,2]

Abstract— **Electrical stimulation of the spinal cord is used for pain relief, and is in use for hundreds of thousands of cases of chronic neuropathic pain. In spinal cord stimulation (SCS), an array of electrodes is implanted in the epidural space of the cord, and electrical currents are used to stimulate nearby nerve fibers, believed to be in the dorsal columns of the cord.**

Despite the long history of SCS for pain, stretching over 30 years, its underlying mechanisms are poorly understood, and the therapy has evolved very little in this time.

Recent work has resulted in the ability to record complex compound action potential waveforms during therapy. These waveforms reflect the neural activity evoked by the therapeutic stimulation, and reveal information about the underlying physiological processes. We aim to simulate these processes to the point of reproducing these recordings.

We establish a hybrid model of SCS, composed of a three-dimensional electrical model and a neural model. The 3D model describes the geometry of the spinal regions under consideration, and the electric fields that result from any flow of current within them. The neural model simulates the behaviour of spinal nerve fibers, which are the target tissues of the therapy. The combination of these two models is used to predict which fibers may be recruited by a given stimulus, as well as to predict the ensuing recorded waveforms.

The model is shown to reproduce major features of spinal compound action potentials, such as threshold and propagation behaviour, which have been observed in experiments.

The model's coverage of processes from stimulation to recording allows it to be compared side-by-side with actual experimental data, and will permit its refinement to a substantial level of accuracy.

I. INTRODUCTION

In SCS therapy, an electrode array is implanted in the epidural space, nestled against the dura. Stimulus currents are applied between electrodes, stimulating nearby nerve fibers. The target tissues are believed to be the Aβfibers in the dorsal columns. These carry tactile information to the brain, and consequently an area of paraesthesia is felt on the body, corresponding to the particular location of the stimulated fibers.

Holsheimer et al. have previously modelled SCS[1], using a volume conductor model of the tissue combined with Frankenhuser-Huxley-McNeal type nerve models. These were used to estimate how many fibers are stimulated, and where these are located. Their work has been used as the foundation of modern SCS research, but they were not able to directly measure spinal nerve recruitment *in vivo*; as a consequence, this important model could not be validated.

[1]J. Laird and J. Parker are with the Graduate School of Biomedical Engineering, University of New South Wales, Kensington NSW 2052, Australia

[2]J. Laird and J. Parker are with National Information and Communications Technology Australia, Eveleigh NSW 2015, Australia {james.laird,john.parker}@nicta.com.au

Technologies have been recently developed that allow the direct recording of spinal cord potentials (SCP), which are evoked during SCS[2]. These represent information about the underlying neurophysiology, as well as the geometry of the sites under stimulation, in ways that are not yet understood.

A number of models of nerve recording exist. For example, Plonsey[3] describes an analytic model of single-neuron recording, while Wijesinghe et al.[4] model the responses seen from propagating action potentials in nerve bundles. However, these models treat fiber stimulation as a fixed property, rather than a nonlinear response to stimulation.

This work aims to build a model that incorporates mechanisms of both stimulation and recording. The basic assumptions of the model are similar to those of Holsheimer's work, extended to consider recordings. New models of tissue and nerves are implemented, using modern data and technologies. The result is a model which is capable of producing the recording waveforms for a given stimulus, as in experiments *in vivo*.

Using recordings from real-world experiments, it is then be possible to close the loop, and refine the model to accurately reproduce the physiological effects of spinal cord neurostimulation.

II. METHOD

A. Therapeutic SCS

The target tissues of SCS are the dorsal columns of the spinal cord, which consist of large numbers of myelinated Aβnerve fibers, oriented along the axis of the spine. These fibers are distinguished by their diameter; the Aβfiber class are amongst the largest of the myelinated nerves, and are considered to comprise fibers in the $7 - 12\,\mu\mathrm{m}$ diameter range. These fibers generally convey touch and kinesthetic information to the brain.

The stimulating electrodes are placed in the epidural space, dorsal to the cord; a commonly used standard array consists of 8 platinum ring electrodes spaced along a flexible silicone tube. The rings are of length 3mm, and spaced on 7mm centres, and the whole array has a diameter of $1.2\,\mathrm{mm}$.

In use, a current waveform is applied between two or more electrodes. This triggers action potentials in nearby nerve fibers, which then propagate along the fibers in both directions. The waveforms used are typically biphasic current pulses; a typical therapy regime might use a $400\,\mu\mathrm{s}$ pulse of between 1 and $30\,\mathrm{mA}$, repeated at $40\,\mathrm{Hz}$.

The resulting action potentials are sustained by ionic flow in and out of the nerve fibers at the nodes of Ranvier, which are regularly spaced points on the fiber where the myelin sheath is interrupted, exposing the active membrane of the

978-1-4577-0216-7/13/$26.00 ©2013 IEEE

fiber. These flows set up an electric field, which can then be measured on other electrodes of the array. The recorded waveform of a single fiber is referred to as a single-fiber action potential (SFAP), while the waveform obtained when multiple fibers are stimulated is a compound action potential (CAP).

B. Neural Model

Each nerve fiber has a cylindrical active membrane, shrouded in an insulating myelin sheath. This sheath is interrupted regularly at the nodes of Ranvier, where the membrane is exposed. These nodes are approximately $2.5\,\mu\mathrm{m}$ long[5], and spaced at approximately 100 times the fiber diameter[6].

The axonal membrane is studded with voltage-gated ion channels, which are exposed to the potential difference between the external medium and the inside of the fiber. Each nerve fiber's behaviour is driven by the electrical field imposed by the stimulation waveform, and as a result currents flow through their membranes at the nodes.

Each fiber is modelled with a lumped cable model, as described by McNeal[5]. The segment between nodes is considered as a conductive cylinder, insulated from the outside, while at each node the membrane's capacitance and ion-channel behaviour determine the currents flowing through the node. The membrane cylinder's diameter is 0.6 of the total fiber diameter[5].

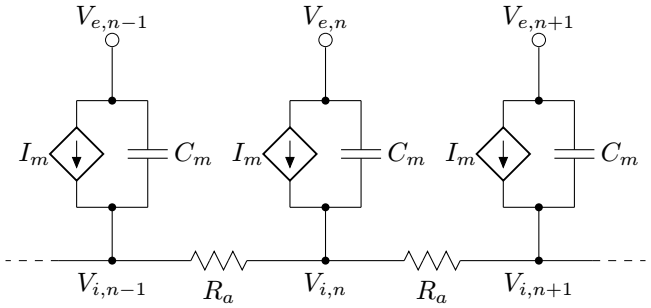

Fig. 1: Lumped cable model of a myelinated nerve fiber, incorporating active ion channel conductance and membrane capacitance at the exposed nodes of Ranvier

The model used for the ion channels of the membrane was derived by Schwarz et al.[7], using measurements from human myelinated nerve fibers. This model incorporates currents corresponding to several sodium and potassium ion channels, as well as a general leakage current across the membrane. It also includes temperature-sensitive terms; for our purposes, we will use the model at 37 degrees Celsius.

Given a set of externally imposed voltage waveforms at the nodes of Ranvier, it is then possible to solve for the resulting current waveforms. This includes the effects of stimulation, as well as any propagating action potentials that may arise. The problem takes the form of a set of ODEs describing the ion channel behaviour at each node, and we solve them using solvers from the GNU Scientific Library[8].

C. Geometric Model

The model consists of a three-dimensional volume conductor model, with compartments of different conductivities. These compartments represent the different tissues of the spinal cord and surrounds. Within each compartment, the tissue is assumed to be homogeneous and linearly conductive. Some tissues may be anisotropic; for example, the white matter of the cord is far more conductive axially than in the transverse direction, due to its being composed of axially oriented fibers, which are not dissimilar to insulating cylinders packed together in a conductive medium. Conductivity figures are taken from Holsheimer et al.[9]

Into the 3D model are incorporated electrodes and nerve fibers. Electrodes may act as current sources, as used to stimulate the nerves; they also act as recording elements for the ensuing evoked potentials. We ground the outer faces of the model, simulating a distant reference electrode.

Nerve fibers are distributed within the white matter in the dorsal column regions. Their nodes of Ranvier are their only electrical connection to the surrounding tissue; as these are so small with respect to the other geometry, we consider them to act as electrical point sources, and to sample the stimulation field at single points.

The current model uses an extruded cross-section to represent the spinal tissues. A representative cross-section of spinal tissue at the T10 level was established from photographs from the Visible Human Project[10], with the neural tissue traced from Nolte et al.[11]. The extrusion length is chosen to be 24cm, with the electrode array axially centred; this arrangement minimses edge effects.

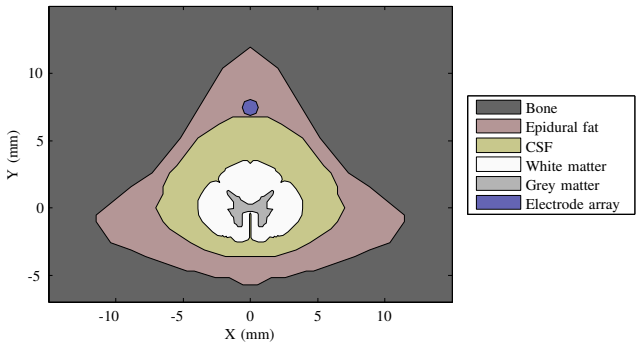

Fig. 2: Cross-section of the extruded model

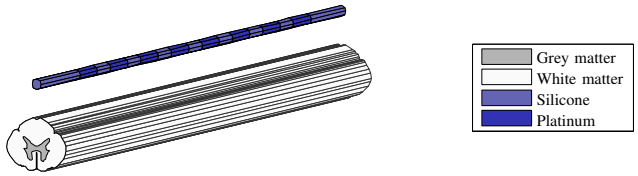

Fig. 3: Placement of the electrode array with respect to the neural tissue

The volume conductor model is used for finite-element simulation of the potential field. The geometry is meshed,

and the simulation engine allows any combination of boundary conditions and current sources to be specified. The solver then returns the potential at all points within the model. Meshing is performed with Tetgen[12], and the finite element solver was written using libMesh[13].

D. Application

Applying the model, once its parameters are determined, is a straightforward process.

1) Stimulus currents result in voltages at nodes of Ranvier on each fiber
2) Fiber response to voltages are calculated
3) Fiber currents result in voltages at electrodes

As mentioned previously, the conductive compartments are all considered to be linear. For a single current source in the volumetric model, the voltage at any point in the space is linearly dependent on the source current. For multiple sources, the voltage at any point is given by the sum of those imposed by each source individually. These properties allow us to express the geometric aspect of the model as a set of transimpedances, relating the voltage at a given point to the current at others.

For an array of m electrodes, and n nodes of Ranvier, we define two transimpedance matrices: F, the forward matrix, and R, the reverse matrix, both of size $m \times n$.

$F_{i,j}$ is the voltage measured at node j for a specific current injected into the model at electrode i. $R_{i,j}$ is the voltage measured at electrode i for a specific current injected into the model at node j.

We use a test current of 1 A and calculate the field in V, so the units of both F and R are Ω.

Given a $1 \times m$ vector of electrode currents I_e, the resulting nodal voltages V_n are given by:

$$V_n = I_e F$$

and similarly, for a $n \times 1$ vector of nodal currents I_n, the electrode voltages V_e are given by:

$$V_e = R V_n$$

This implies that we can use the (expensive) finite-element model to calculate the values of F and R just once, and then apply different stimulation waveforms $I_e(t)$ and receive the appropriate recordings $V_e(t)$.

E. Interpolation

A naïve implementation of this model would run the finite element model $m + n$ times - applying a test current through each electrode in turn whilst collecting the nodal voltages into F, and then vice versa into R. While m is typically small, n can be on the order of 10^6 in a model with 1000 fibers. Given the typical expense of a finite-element simulation - taking several minutes on a modern computer - it is not practical to run the simulation for each element of R individually.

Instead, we take advantage of the nodes' proximity to each other, and the spatial smoothness of the reverse transimpedance with respect to node position. We select sampling points distributed within the white matter space, taking care to include all regions in which nerve nodes are distributed. A simulation is performed sourcing a current from each sampling point, and the results are interpolated using natural neighbour interpolation to yield the values of R for each node according to its position.

This approach limits the computational complexity of the geometric modelling to the number of sampling nodes, independent of fiber parameters. The number of nodes is chosen to achieve an insubstantial error in the interpolated values. For the model described here, 5000 nodes within the white matter region were chosen, and 500 nodes were located on the surface of the compartment.

III. RESULTS

A simulations was carried out with the described geometry. 1000 fibers were distributed uniformly within the dorsal column region of the spinal cord, shown in Figure 4. Their diameters are generated using a normal distribution, with parameters described in Table I.

Parameter	Value
Number	1000
Range	$1 - 15\,\mu$m
Mean	$10\,\mu$m
Standard Deviation	$3\,\mu$m

TABLE I: Fiber diameter distribution used in simulation

Stimulation consisted of bipolar, monophasic current pulses, ranging in amplitude from 1 to 10 mA in 1 mA steps and with a duration of 200 μs. Single pulses were delivered on electrodes 1 and 2, and the ensuing potentials recorded on electrodes 3 through 8.

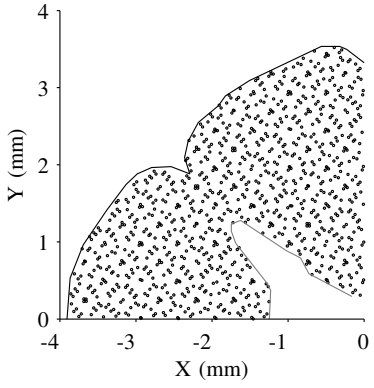

Fig. 4: Distribution of fibers within the white matter

With low stimulation currents, we do not observe a response. As the stimulation current is increased, a threshold point is reached at which responses start to be observed on all measuring electrodes. From this point on, the response varies with the applied current. A peak-to-peak measure of the response size on several electrodes is shown in Fig. 5c.

In the recorded waveforms (Figure 5a), we observe the characteristic tri-lobed shape of spinal compound action

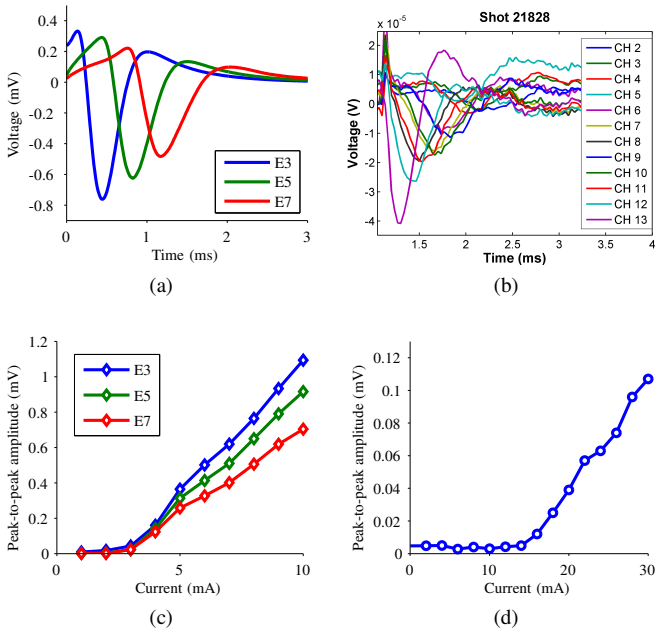

Fig. 5: Results of simulation. (a): the recorded waveform from several electrodes along the array for a stimulation current of 5mA. (b): an example recorded waveform from a human subject, reproduced from [14]. Note that the timebase differs from (a). (c): the peak-to-peak amplitude of the waveform on electrodes 3, 5 and 7 for all currents. (d): some example peak-to-peak growth curves from a second human subject, reproduced from [2]

potentials, as seen in humans. These three lobes are referred to as the P1, N1, and P2 peaks, in that order. Looking at several electrodes after a single stimulus, as in Fig. 5a, we see that the signal is delayed on successively more distant electrodes, as the action potential volley takes longer to travel past them. Their amplitude also decreases and their waveforms widen, due to the dispersion caused by the range of fiber diameters involved - the propagation velocity of a fiber increases in proportion to its diameter, while the width of its waveform decreases.

For comparison, we present a single recording from a human spinal cord at lower amplitude in Figure 5b; despite the presence of large amounts of noise and exponential artifact from stimulation, we see a similar decay in envelope amplitude with distance, and the tri-lobed shape of the signal.

We also reproduce some current growth curves measured in a human in Figure 5d, showing the threshold behaviour and linear dependence of the peak-to-peak response amplitudes on current.

IV. DISCUSSION

We observe many of the key features of recordings from human subjects. The relationship between current and recording amplitude is essentially linear above threshold, and the waveforms tend to spread and decay in amplitude as they propagate past successive electrodes. While no effort has been made to tune parameters to accurately reproduce specific *in vivo* recordings, this nonetheless suggests that the model is capable of reproducing salient features of the relevant physiological systems.

This model begins to describe the many features observed in SCS recordings from human subjects. These recordings provide an unprecedented window into what happens after stimulation, and this model is the first attempt to explain their origins. It is both computationally tractable and flexible, and is the first model of SCS which can be compared directly to objective measurements.

Further work with this model will permit the development of improved therapeutic systems, including novel stimulation regimes, electrode designs, and feedback algorithms, with the aim of improving pain therapy outcomes.

REFERENCES

[1] J. J. Struijk, J. Holsheimer, B. K. V. van, and H. B. Boom, "Epidural spinal cord stimulation: calculation of field potentials with special reference to dorsal column nerve fibers," *IEEE Transactions on Biomedical Engineering*, vol. 38, no. 1, pp. 104–110, 1991. [Online]. Available: http://doc.utwente.nl/15340/

[2] J. L. Parker, D. M. Karantonis, P. S. Single, M. Obradovic, and M. J. Cousins, "Compound action potentials recorded in the human spinal cord during neurostimulation for pain relief," *PAIN*, vol. 153, no. 3, pp. 593 – 601, 2012. [Online]. Available: http://www.sciencedirect.com/science/article/pii/S0304395911006993

[3] R. Plonsey, "The active fiber in a volume conductor," *IEEE Trans Biomed Eng*, vol. 21, no. 5, pp. 371–381, Sep 1974.

[4] R. S. Wijesinghe, F. L. Gielen, and J. P. Wikswo, "A model for compound action potentials and currents in a nerve bundle. I: The forward calculation," *Ann Biomed Eng*, vol. 19, no. 1, pp. 43–72, 1991.

[5] D. R. McNeal, "Analysis of a model for excitation of myelinated nerve," *IEEE Trans Biomed Eng*, vol. 23, pp. 329–337, Jul 1976.

[6] R. L. Friede, J. Brzoska, and U. Hartmann, "Changes in myelin sheath thickness and internode geometry in the rabbit phrenic nerve during growth," *J. Anat.*, vol. 143, pp. 103–113, Dec 1985.

[7] J. R. Schwarz, G. Reid, and H. Bostock, "Action potentials and membrane currents in the human node of ranvier." *Pflugers Arch*, vol. 430, no. 2, pp. 283–292, 1995.

[8] M. Galassi, J. Davies, J. Theiler, B. Gough, G. Jungman, M. Booth, and F. Rossi, *Gnu Scientific Library: Reference Manual*. Network Theory Ltd., Feb. 2003.

[9] J. J. Struijk, J. Holsheimer, B. K. van Veen, and H. B. Boom, "Epidural spinal cord stimulation: calculation of field potentials with special reference to dorsal column nerve fibers," *IEEE Trans Biomed Eng*, vol. 38, pp. 104–110, Jan 1991.

[10] M. Ackerman, "The visible human project," *Proceedings of the IEEE*, vol. 86, no. 3, pp. 504–511, March 1998.

[11] J. Nolte and J. B. Angevine, *The Human Brain: in Photographs and Diagrams*, 2nd ed. Mosby, 2000.

[12] H. Si, "TetGen: A Quality Tetrahedral Mesh Generator and Three-Dimensional Delaunay Triangulator," http://tetgen.berlios.de/. [Online]. Available: http://tetgen.berlios.de/

[13] B. S. Kirk, J. W. Peterson, R. H. Stogner, and G. F. Carey, "libmesh: a c++ library for parallel adaptive mesh refinement/coarsening simulations," *Eng. with Comput.*, vol. 22, no. 3, pp. 237–254, Dec. 2006. [Online]. Available: http://dx.doi.org/10.1007/s00366-006-0049-3

[14] J. L. Parker, D. M. Karantonis, P. S. Single, M. Obradovic, J. H. Laird, R. B. Gorman, N. H. Shariati, M. Bickerstaff, and M. J. Cousins, "Measuring Spinal Cord Potentials," 2012, 16th Annual Meeting of the North American Neuromodulation Society.